

BIZARRE HARD X-RAY OUTBURSTS OF CYGNUS X-1

BORIS E. STERN,^{1,2} ANDREI M. BELOBORODOV,¹ AND JURI POUTANEN
 Stockholm Observatory, SE-133 36, Saltsjöbaden, Sweden; {stern, andrei, juri@astro.su.se}

The Astrophysical Journal, in press

ABSTRACT

A very high activity of Cygnus X-1 on 1999 April 19-21 was recorded by BATSE Large Area Detectors onboard the *Compton Gamma-Ray Observatory (CGRO)*. The peak luminosity was one order of magnitude higher than the normal luminosity of Cyg X-1. This fact can be critical for models of the hard state of Cyg X-1. The longest outburst lasted ~ 1000 s and demonstrated very unusual temporal and spectral behavior which indicates the presence of two emission components. One component is relatively soft (with a cutoff below ~ 100 keV) and highly variable, and the other one is hard (extending above 100 keV), with much slower variability.

Subject headings: accretion, accretion disks – gamma-rays: observations – stars: individual (Cygnus X-1)

1. INTRODUCTION

Cyg X-1 is a persistent X-ray source believed to be powered by accretion onto a black hole from a massive companion. Most of the time Cyg X-1 spends in the hard state and sometimes it switches to the soft state (see, e.g., Liang & Nolan 1984; Zhang et al. 1997; Poutanen 1998; Gierliński et al. 1999). The X-ray luminosity above ~ 2 keV is estimated to be about 3×10^{37} erg s⁻¹ (Gierliński et al. 1997), assuming the distance to the source, $D = 2$ kpc (Massey, Johnson, & DeGioia-Eastwood 1995; Malysheva 1997).

Variability of Cyg X-1 was extensively studied with various instruments (see, e.g., Ling et al. 1987; Gilfanov et al. 1995; Phillips et al. 1996; Kuznetsov et al. 1997; Paciesas et al. 1997; Wen et al. 1999; Brocksopp et al. 1999; Bałucińska-Church et al. 2000). These studies show the stability of the hard state of Cyg X-1. The photon flux above 50 keV is normally ~ 0.1 ph cm⁻² s⁻¹ with variations by a factor 2.

In this Letter, we analyze the period of the unusually strong hard X-ray activity of Cyg X-1 on 1999 April 21. Two strong outbursts activated the BATSE/CGRO (Fishman et al. 1989) onboard trigger. We analyze the temporal structure of the outbursts in the four LAD energy channels 1–4, estimate the peak luminosity of Cyg X-1, and discuss possible implications for theoretical models of accretion in this object.

2. THE OUTBURSTS

The unusual activity of Cyg X-1 can be traced back to 1999 April 19 (TJD 11287). Two events recorded on April 19 were found in the BATSE data during search for non-triggered gamma-ray bursts (GRBs) (Stern et al. 1999, 2000a). The best fit locations were within $4^\circ - 5^\circ$ from Cyg X-1 (1σ errors exceeded 10° for those events). We use the location procedure described in Stern et al. (2000b) which is similar to that used for GRB location by Pendleton et al. (1999). The estimated peak fluxes above 50 keV were about 0.3 and 0.5 ph cm⁻² s⁻¹ which is high as compared with the normal flux from Cyg X-1. On April 20, BATSE detectors were triggered by another event with right ascension, $\alpha = 305^\circ 1$, and declination, $\delta = 26^\circ 2$ (BATSE estimate, note also that this event is identified as a

GRB in the BATSE data base). Again, the location was close to Cyg X-1 (slightly beyond 1σ error circle).³ The peak flux of this event was about 0.5 ph cm⁻² s⁻¹.

On April 21, the two brightest outbursts occurred, with the interval ~ 2.5 hours. Between and after the two outbursts, Cyg X-1 demonstrated nothing unusual, being in the hard state with normal luminosity. The summary of all the five events is given in Table 1.

We will concentrate on the two brightest events on April 21 (two last lines in Table 1). The locations of both events coincide with the location of Cyg X-1 with 2° accuracy. In principle, it might be accidental projections of GRBs on Cyg X-1. The probability that one of $\sim 10^3$ detected GRBs with comparable brightness will appear within 2° from Cyg X-1 is about 0.3. However, the probability of appearance of two such GRBs from the same location within 2.5 hours is low, $\sim 10^{-5}$. Besides, the long duration of the events, $\sim 10^3$ s, is very unusual for GRBs. One concludes that the events are outbursts of Cyg X-1.

TABLE 1
 SUMMARY OF OUTBURSTS ON 1999 APRIL 19 - 21

ST2000 ^a	# ^b	time ^c , s	α ^d	δ ^d	1σ ^d
11287a	...	16816	297.8	38.2	18.4
11287b	...	18071	296.6	38.0	12.9
11288e	7523	83437	305.6	27.6	6.0
11289c	7524	54530	299.9	34.4	2.4
11289e	7525	63100	298.4	35.2	1.2

^a Name in the catalog of Stern et al. (1999), consisting of TJD and a letter.

^b BATSE trigger number.

^c Time of the day in seconds.

^d The best fit location and its 1σ error (deg).

2.1. Outburst 11289c

The first outburst on April 21 has similar light curves in LAD energy channels 1–3 (see top panel in Fig. 1). The signal in channel 4 (above 300 keV) was low, practically undetectable. The signal was cut off by Earth occultation at ≈ 55.23 ks. We model the background during the outburst using a linear fit extrapolating the background after the occultation.

¹Also at Astro-Space Center of Lebedev Physical Institute, Profsoyuznaya 84/32, 117810 Moscow, Russia

²Also at Institute for Nuclear Research, Russian Academy of Sciences, 117312 Moscow, Russia

³The coordinates of Cyg X-1 are $\alpha = 299^\circ 5$ and $\delta = 35^\circ 2$.

In order to get the photon and energy fluxes, we fit the signal count rate in the three energy channels using the detector response matrix computed with the code of Pendleton (see Pendleton et al. 1999 and references therein). An exponentially cutoff power-law is assumed as a spectral hypothesis. The photon and energy fluxes are then obtained by integrating the best fitting spectrum in the proper energy band. The error is estimated to be about 15%. (Note that the overall systematic error in the BATSE flux normalization may be about 20%, see, e.g., Much et al. 1996.)

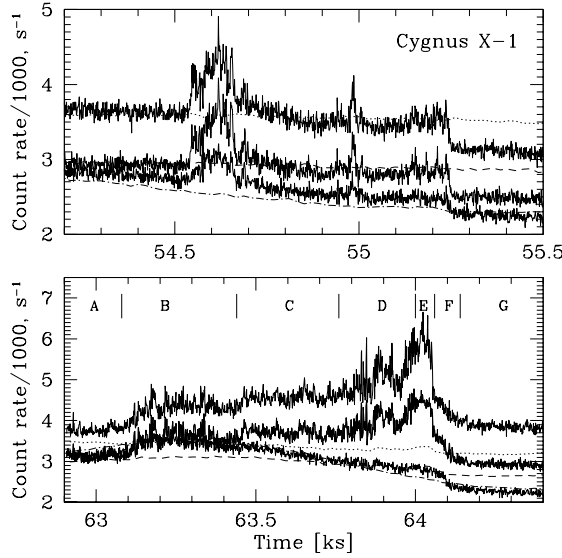


FIG. 1.— Count rate during the two outbursts of Cyg X-1 on 1999 April 21 (TJD 11289) in the three LAD energy channels, 1–3. The count rate is summed over two detectors closest to the line of sight to Cyg X-1. Count rates are higher in softer channels. Dotted, dashed and dot-dashed curves show the background in channels 1, 2, and 3, respectively, as seen by two detectors looking away from Cyg X-1.

TABLE 2
PEAK FLUXES AND LUMINOSITIES

Outburst	$F_{>50}^a$	$F_{>30}^b$	$L_{>50}^c$	$L_{>30}^d$
11289c	1.1	2.4	0.75×10^{38}	1.2×10^{38}
11289e	1.3	3.9	0.8×10^{38}	1.6×10^{38}

^a Peak flux ($\text{ph cm}^{-2} \text{s}^{-1}$) above 50 keV.

^b Peak flux above 30 keV.

^c Peak luminosity (erg s^{-1}) above 50 keV (assuming distance $D = 2 \text{ kpc}$).

^d Peak luminosity above 30 keV.

The peak flux in 50–300 keV band (channels 2–3) is about $1.1 \text{ ph cm}^{-2} \text{s}^{-1}$ which is ~ 10 times higher than the normal flux from Cyg X-1. The flux averaged over hundred seconds (54.55–54.65 ks interval) is $0.75 \text{ ph cm}^{-2} \text{s}^{-1}$. The peak luminosity above 30 keV exceeds $10^{38} \text{ erg s}^{-1}$ (see Table 2 for details). Note that the strong increase in the luminosity was not accompanied by crucial changes in the spectrum. At least, the hardness ratios during the outburst stayed similar to the normal hard state of Cyg X-1 (see § 3).

2.2. Outburst 11289e

The second outburst on April 21 was detected ~ 8 ks after the first outburst (see bottom panel in Fig. 1). Unfortunately, there is a gap in the data at the time when Cyg X-1 rose above the horizon (~ 62.8 ks). The data records start at ≈ 62.9 ks. Note that there was no occultation of Cyg X-1 in the end of the

outburst. The sharp fall off in the light curves in each channel is the intrinsic behavior of the source. It allows one to estimate the peak flux and luminosity of the outburst which we give in Table 2. The corresponding luminosities averaged over interval E (see Fig. 1) are 20% smaller than the peak values.

The ionospheric background showed smooth latitude variations during the outburst (see bottom panel of Fig. 1) on the time-scale of order 1 ks. The background level is different in different detectors, therefore, it is difficult to extract exactly the signal seen in the detectors looking at Cyg X-1. The signal uncertainty caused by the background variations is of order 20%.

One can get a good location fit for the signal by analyzing the variable part of the light curve. At a given time interval, we fit the light curve by a linear function and take it as a “reference” level. (It thus includes both the background and the linear part of the true signal.) We then take the difference between the count rate (at this or another interval) and the reference level as a “signal”. The location fits demonstrate that almost all variable part of the signal comes from the direction of Cyg X-1 with $\sim 5^\circ$ accuracy at all time intervals A–F marked in Figure 1 (see Table 3). The residual signal can be fitted by 200 s–400 s long linear fragments with a good χ^2 (lines 1–3 in Table 3). This means that no fraction of the variable signal can be mimicked by magnetospheric phenomena like particle precipitation which either produces a diffuse flux of photons or can be a localized source at some distance from the spacecraft. In the first case the location fit is so bad that the residual χ^2 is comparable to the initial one, and in the second case one observes a fast change in the direction of the source due to the satellite motion. In our case, the satellite moved ~ 6000 km between intervals B and E, while the source’s position on the sky did not change.

TABLE 3
LOCATION FITS FOR DIFFERENT TIME INTERVALS

Signal ^a	Reference ^b	Channel	α^c	δ^c	$1\sigma^c$	χ_0^2/χ_r^2 ^d
B	B	2+3	302.1	37.1	6.6	11.4 / 0.93
D+E	D+E	1	302.3	38.4	2.0	34.0 / 1.13
D+E	D+E	2+3	301.3	40.2	6.0	16.9 / 1.05
D+E	G	2+3	298.4	35.2	1.2	44.7 / 10.8
E	E	1	303.9	40.1	4.9	15.3 / 0.90
E+F	G	3	298.8	33.5	2.1	64.4 / 2.35
F	G	2+3	302.4	40.3	4.1	51.0 / 1.66

^a The time interval in which the location fit is done for the residuals after subtracting a linear (“reference”) function from the count rate.

^b The interval at which the linear reference function was fitted.

^c The best fit location and its 1σ error (deg).

^d χ_0^2 and χ_r^2 are χ^2 per dof for the count rate relative to the reference level and for the residual signal after the location fit, respectively.

While the first April 21 outburst is unusual only for its strength, the second one is even more surprising. The behavior of the light curve in different energy channels suggests the presence of two independent emission components. The first (highly variable) component dominates the signal in channels 1 and 2, and the second component (with low amplitude of variability) dominates the signal in channel 3. The soft component terminated at 64.05 ks and then one observes only the hard component in the three channels. Unfortunately, the spectral data for this outburst were lost, which did not allow us to confirm the two-components by spectral analysis.

Since we cannot exactly separate the signal from the background, we study the outburst using the strong non-Poisson variability produced by the signal in the count rate. In each time interval, A–F, we compute the root-mean-square (rms) of

the signal variations, S_i , around the linear fits ($i = 1, 2, 3$ is the channel number). We then compute the “fluctuation hardness ratio”, fhr, that is the ratio of the rms in different channels. The rms (with subtracted Poisson component) and $\text{fhr}_{21} \equiv \text{rms}_2/\text{rms}_1$ are given in Table 4. Assuming the rms to be roughly proportional to the average level of the signal, the fhr may give an estimate for the true hardness ratio. The decrease of the fhr_{21} as the outburst progresses indicates that the variable component gets softer.

TABLE 4
CHARACTERISTICS OF THE COUNT RATE VARIABILITY

Interval	rms_1	rms_2	rms_3	c_{23}	fhr_{21}
A	97	109	70	0.63 ± 0.09	1.12 ± 0.06
B	300	316	169	0.92 ± 0.02	1.05 ± 0.02
C	211	213	96	0.77 ± 0.05	1.01 ± 0.03
D	499	370	100	0.71 ± 0.04	0.74 ± 0.01
E	568	286	90	0.15 ± 0.07	0.50 ± 0.02
F	109	196	106	0.92 ± 0.07	1.32 ± 0.10

The 1σ errors of c_{23} and fhr_{21} are of Poisson nature; they are estimated with the bootstrap method. The measured hardness ratios are not affected by the background uncertainty because they are based on the signal dispersion in a narrow time interval where the background is almost linear.

We then compute the cross-correlation coefficient between channels 2 and 3, $c_{23} \equiv (\langle S_2 \cdot S_3 \rangle - \langle S_2 \rangle \langle S_3 \rangle) / (\text{rms}_2 \text{rms}_3)$ (see Table 4). The cross-correlation decreases during the outbursts and becomes very low in interval E. It confirms that the soft component gets so soft that it practically does not contribute to the signal in channel 3. In interval F, the cross-correlation is high, confirming that the soft component has disappeared and we see only the second (hard) component in all the three channels. The luminosities of the soft and hard components can be roughly estimated from the step-like cut offs at 64.05 ks and 64.1 ks, respectively. The average luminosity of Cyg X-1 in time interval E above 50 keV (30 keV) is $L_{>50} \sim 2.5 \times 10^{37} \text{ erg s}^{-1}$ ($L_{>30} \sim 7.0 \times 10^{37} \text{ erg s}^{-1}$) in the soft component and $L_{>50} \sim 4.0 \times 10^{37} \text{ erg s}^{-1}$ ($L_{>30} \sim 5.5 \times 10^{37} \text{ erg s}^{-1}$) in the hard component.

3. COMPARISON WITH THE NORMAL HARD STATE OF CYG X-1

The normal hard state of Cyg X-1 was studied using the Earth occultations which occur on each orbit of the *CGRO*. The step in the light curve at the moment of occultation shows the amplitude of the signal from Cyg X-1 in each energy channel. The study of Cyg X-1 with this method was done by Ling et al. (1997) and Paciesas et al. (1997). We performed a similar analysis for ~ 60 occultations and evaluated the flux from Cyg X-1 and the hardness ratio hr_{32} (ratio of the signal count rates in channels 3 and 2) for each occultation. The results are shown in Figure 2. The observed large dispersion in the hardness ratio may be caused by the measurement errors rather than intrinsic variability of Cyg X-1. To estimate the errors we did a similar analysis of 80 occultations of the Crab nebula which is known to be a steady source. We found $\text{hr}_{32} = 0.66 \pm 0.13$ and the count rate 316 ± 110 , where the errors represent the standard deviations. The major cause of the errors is the uncertainty in the changing background (to have good statistics one has to fit the signal on a relatively long period ~ 100 s before and after the occultation, and the background curvature plays a role). One should note that the error in the hardness ratio of Cyg X-1 is likely to be smaller than that for the Crab since its flux is larger. In the outbursts, these errors are even smaller.

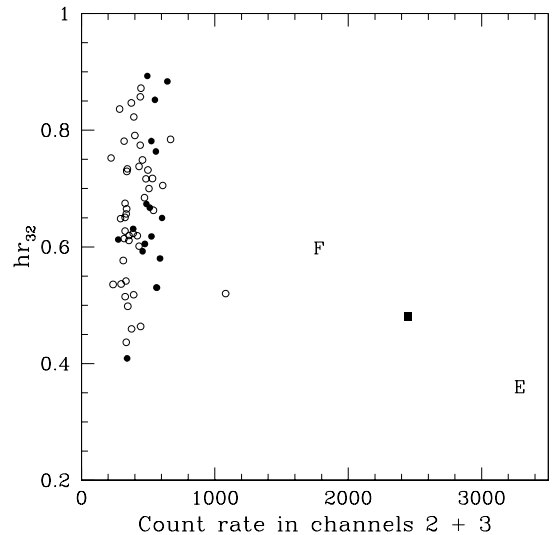


FIG. 2.— Hardness ratio, hr_{32} , of the signal count rates in channels 3 and 2 versus count rate in channels 2+3, as measured in all detectors (note the difference from Fig. 1 where the count rate is given only for two detectors). *Open circles* show a sample of occultations in the period TJD 8600–8700; *filled circles* show the same in the period TJD 9990–10000. Cyg X-1 was in the normal hard state with relatively high brightness in both periods. The dispersion in hr_{32} may be caused by measurement errors (see the text). *Filled square* corresponds to the first outburst on April 21 (between 54.55 and 54.65 ks). Labels F and E represent the second outburst on April 21 in time intervals F and E, respectively. (The signal was roughly estimated by subtracting the level of the count rate in interval G.)

For comparison we also show the estimates of the flux and hardness ratio for the two April 21 outbursts. Note that outburst 11289c and interval F of outburst 11289e have hardness ratios similar to the normal hard state. Interval E of outburst 11289e is significantly softer.

The presence of two emission components (soft, highly variable, and hard, with lower variability) in outburst 11289e is intriguing. Are they present in the normal state of Cyg X-1? In the sample of 63 occultations we found that the fractional rms of the count rate (i.e. the ratio of the rms to the mean count rate) in channel 2 was higher than that in channel 3 in 47 cases. This indicates higher variability in channel 2 (the probability of such an accidental excess is $0.5 \cdot 10^{-4}$). The decreasing of the variability with energy was also observed in the 2–40 keV band (Nowak et al. 1999; Revnivtsev et al. 2000). These facts are consistent with the presence of a hard component with a low variability though this interpretation is not unique. Note also that Gierliński et al. (1997) got the best fit to the broad-band X-ray spectrum of Cyg X-1 with two thermal Comptonization components of different temperatures.

4. DISCUSSION

The hard state of Cyg X-1 has been a puzzle since its discovery. The standard accretion disk model (Shakura & Sunyaev 1973) was not able to explain the X-ray spectrum, and two modifications of the model were suggested: a two-temperature hot disk and an active corona atop the standard disk (see Beloborodov 1999a for a recent review).

The advective hot-disk models (e.g. Esin et al. 1998) are consistent with the observed spectrum and luminosity of Cyg X-1 if the accretion rate has a specific value $\dot{M} \approx \dot{M}_{\text{max}} \approx 10\alpha^2 L_E/c^2$ and the viscosity parameter $\alpha \approx 0.2 - 0.3$. Here $L_E = 4\pi c G M m_p / \sigma_T = 1.3 \times 10^{39} (M/10M_\odot) \text{ erg s}^{-1}$ is the Eddington luminosity. Small variations in the accretion rate,

$\Delta\dot{M}/\dot{M} \sim 10\%$, were predicted to destroy the hard state (Esin et al. 1998; but see also Zdziarski 1998). By contrast, the luminosity of Cyg X-1 is known to vary by a factor of two without substantial changes in the spectral shape (e.g., Paciesas et al. 1997; Gierliński et al. 1997). Such fluctuations already challenged the model, and the hard outbursts analyzed in this Letter are even more difficult to explain. The model would work only assuming a specific dependence $\alpha \propto \dot{M}^{1/2}$ that keeps $\dot{M} \approx \dot{M}_{\max}$; α then should be about unity at the peak of the outburst.

In the context of the disk-corona model, the outbursts can be interpreted as an enhanced coronal activity of the accretion disk. In this model, the X-ray spectral slope is controlled by one parameter, the feedback factor due to X-ray reprocessing by the disk. The hard-state spectrum of Cyg X-1 is well explained if the coronal plasma is ejected away from the disk with a mildly relativistic velocity $\beta = v/c \sim 0.3$ (Beloborodov 1999b; Malzac, Beloborodov, & Poutanen 2001). Alternatively, the observed emission may be produced by a static corona atop a strongly ionized disk (e.g., Ross, Fabian, & Young 1999; Nayakshin 1999). The corona becomes e^\pm -dominated at high luminosities and its temperature decreases (e.g., Svensson 1984; Stern et al. 1995; Poutanen & Svensson 1996). Pair creation may cause the shift of the spectral break in outburst 11289e to smaller energies.

Cyg X-1 is a massive X-ray binary and it may be fed mainly by the donor wind. Then the pattern of accretion can change completely compared to the standard viscous α -disk or its modifications. The captured wind matter has a low angular momentum, just about critical for disk formation (Illarionov & Sunyaev 1975). Under such conditions, a small-scale inviscid disk forms, which accretes super-sonically (Beloborodov & Illarionov 2001). The disk forms in the ring-like caustic of the accretion flow where energy is liberated in inelastic collision of gas streams. A Comptonized power-law spectrum is then emitted with a standard break at ~ 100 keV, and it has appearance

of a normal hard state of Cyg X-1.

The two-component emission in outburst 11289e probably requires a two-zone emission model. For instance, the soft component may be associated with a variable coronal emission atop the disk, and the hard component with an inner relativistic jet. A corona-jet model was recently proposed by Brockopp et al. (1999) based on correlations between the X-rays and the radio emission observed in Cyg X-1. The April 1999 outbursts were, however, too short to have a significant impact on the flux in radio and no substantial changes were detected (R. Fender and G. Pooley, private communication). In the context of the wind-fed accretion model, the two-component emission can naturally appear if viscous accretion disk and wind-disk collision are both operating in the source.

Concluding, the 1999 April 21 outbursts are the brightest events detected from Cyg X-1 by BATSE during 9 years of its operation. The hard X-ray luminosity above 30 keV was in excess of 10^{38} erg s $^{-1}$. Unfortunately, there are no simultaneous observations in the soft X-rays, so that one can only guess what was the total luminosity. The large luminosity and unusual spectral behavior challenge the theoretical models of accretion in Cyg X-1.

We thank Rob Fender, Guy Pooley, and Jerry Bonnell for useful discussions. We are grateful to Rob Preece and Geoff Pendleton for providing the code for computing the detector response matrix and an anonymous referee for useful comments that significantly improved the paper. This research has made use of data obtained through the High Energy Astrophysics Science Archive Research Center Online Service, provided by the NASA/Goddard Space Flight Center. This work was supported by the Swedish Natural Science Research Council, the Swedish Royal Academy of Sciences, the Wenner-Gren Foundation for Scientific Research, the Anna-Greta and Holger Crafoord Fund, and RFBR grant 00-02-16135.

REFERENCES

Baucińska-Church, M., Church, M. J., Charles, P. A., Nagase, F., LaSala, J., & Barnard, R. 2000, MNRAS, 311, 861

Beloborodov, A. M. 1999a, in ASP Conf. Ser. 161, High Energy Processes in Accreting Black Holes, ed. J. Poutanen, R. Svensson (San Francisco: ASP), 295

Beloborodov, A. M. 1999b, ApJ, 510, L123

Beloborodov, A. M., & Illarionov, A. F. 2001, MNRAS, in press (astro-ph/0006351)

Brockopp, C., Fender, R. P., Larionov, V., Lyuty, V. M., Tarasov, A. E., Pooley, G. G., Paciesas, W. S., Roche, P. 1999, MNRAS, 309, 1063

Esin, A. A., Narayan, R., Cui, W., Grove, J. E., & Zhang, S.-N. 1998, ApJ, 505, 854

Fishman, G. J., et al. 1989, Proc. Gamma Ray Observatory Science Workshop, ed. W. N. Johnson (Greenbelt: Goddard Space Flight Center), 3-47

Gierliński, M., Zdziarski, A. A., Done, C., Johnson, W. N., Ebisawa, K., Ueda, Y., Haardt, F., & Phlips, B. F. 1997, MNRAS, 288, 958

Gierliński, M., Zdziarski, A. A., Poutanen, J., Coppi, P. S., Ebisawa, K., & Johnson, W. N. 1999, MNRAS, 309, 496

Gilfanov, M. et al. 1995, in NATO C 450, The Lives of the Neutron Stars, ed. M. A. Alpar et al. (Dordrecht: Kluwer Academic Publishers), 331

Illarionov, A. F., & Sunyaev, R. A. 1975, A&A, 39, 185

Kuznetsov, S., et al. 1997, MNRAS, 292, 651

Liang, E. P., & Nolan, P. L. 1984, Space Sci. Rev., 38, 353

Ling, J. C., Mahoney, W. A., Wheaton, Wm. A., & Jacobson, A. S. 1987, ApJ, 321, L117

Ling, J. C., et al. 1997, ApJ, 484, 375

Malysheva, L. K. 1997, Astron. Lett., 23, 585 [in Russian: PAZh, 23, 667]

Malzac, J., Beloborodov, A. M., & Poutanen, J. 2001, MNRAS, in press (astro-ph/0102490)

Massey, P., Johnson, K. E., & DeGioia-Eastwood, K. 1995, ApJ, 454, 171

Much, R., et al. 1996, A&AS, 120, 703

Nayakshin, S. 1999, in ASP Conf. Ser. 162, Quasars and Cosmology, ed. G. Ferland, J. Baldwin (San Francisco: ASP), 87

Nowak, M. A., Vaughan, B. A., Wilms, J., Dove, J. B., & Begelman, M. C. 1999, ApJ, 510, 874

Paciesas, W. S., Robinson, C. R., McCollough, M. L., Zhang, S. N., Harmon, B. A., Wilson, C. A. 1997, in AIP Conf. Proc. 410, Proc. of the 4th Compton Symposium, ed. C. D. Dermer, M. S. Strickman, & J. M. Kurfess (New York: AIP), 834

Pendleton, J. N., et al. 1999, ApJ, 512, 362

Phlips, B. F., et al. 1996, ApJ, 465, 907

Poutanen, J. 1998, in Theory of Black Hole Accretion Disks, ed. M. A. Abramowicz, G. Björnsson, & J. E. Pringle (Cambridge: Cambridge Univ. Press), 100

Poutanen, J., & Svensson, R. 1996, ApJ, 470, 249

Revnivtsev, M. G., Borozdin, K. N., Priedhorsky, W. C., & Vikhlinin, A. 2000, ApJ, 530, 955

Ross, R. R., Fabian, A. C., & Young, A. J. 1999, MNRAS, 306, 461

Shakura, N. I., & Sunyaev, R. A. 1973, A&A, 24, 337

Stern, B. E., Poutanen J., Svensson, R., Sikora, M., & Begelman, M. C. 1995, ApJ, 449, L13

Stern, B. E., Tikhomirova, Ya., Kompaneets, D., Stepanov, M., Berezhnoy, A., & Svensson, R. 1999, in ASP Conf. Ser. 190, Gamma-Ray Bursts: The First Three Minutes, ed. J. Poutanen, R. Svensson (San Francisco: ASP), 253

Stern, B. E., Tikhomirova, Ya., Stepanov, M., Kompaneets, D., Berezhnoy, A., & Svensson, R. 2000a, ApJ, 540, L21

Stern, B. E., Tikhomirova, Ya., Kompaneets, D., Svensson, R., & Poutanen, J. 2000b, ApJ, submitted (astro-ph/0009447)

Svensson, R. 1984, MNRAS, 209, 175

Wen, L., Cui, W., Levine, A. M., & Bradt, H. V. 1999, ApJ, 525, 968

Zdziarski, A. A. 1998, MNRAS, 296, L51

Zhang, S. N., Cui, W., Harmon, B. A., Paciesas, W. S., Remillard, R. E., & van Paradijs, J. 1997, ApJ, 477, L95